# Supplementary Information for

## Anomalies in Supercooled Water at ~230 K Arise from a 1D Polymer to 2D Network Topological Transformation

Saber Naserifar, William A. Goddard III.

Correspondence to: wag@caltech.com

**This PDF file includes:**

1. Methods
2. Primitive Ring Analysis
3. Ring Structures of Supercooled Water at Different Temperatures
4. Number of Rings of Supercooled Water at Different Temperatures
5. Structural Ordering as a Function of Temperature
6. Structural Analysis of Supercooled Water at 140 K
7. Diffusivity Calculations for Supercooled Water
8. Hydrogen Bond Lifetime Using Empirical Models
9. Population Analysis of Different Ring Sizes
10. Lifetime of Different Ring Sizes
11. References for SI Reference Citations

Figs. S1 to S12

Tables S1 to S2

## 1. Methods

**MD Simulations.** All simulations were carried out using the RexPoN FF with rigid water model except for diffusivity calculations given in Figure 5 in which we used flexible heavy water ($D_2O$) (see section 7 for discussion). The mathematical formulation of RexPoN, training set, optimization process, and complete list of parameters are provided separately[1]. We integrated the RexPoN FF into the LAMMPS[2] molecular dynamics simulator package, which we used for all simulations. All simulations used periodic cells with 216 rigid molecules. All supercooling simulations were carried out in the *NVT*-MD ensemble along the 1 atm density line. The experimental densities were used for temperatures above 240 K while for temperatures below 240 K, we used the moderate density extrapolation proposed by Kim *et al.* [3]. For each density, we first equilibrated the system at 300 K for 1 ns. Then, the system was cooled down during a step-by-step process to 260, 250, 240, 235, 232, 230, 228, 225, 220, 210, and 200 K. At each temperature the system was relaxed for 0.5 ns before going to the next temperature. The simulation time step was 1.0 fs. To control the temperature we used the Nosé-Hoover thermostat with a relaxation time of 100 fs[4].

**2PT Analysis.** We calculated the thermodynamic response and the phase transition properties by computing the Helmholtz free energy $A$ and the entropy $S^0$ using the 2PT technique[5-6]. 2PT uses the Fourier transform of the velocity autocorrelation function to determine the vibrational density of states after which corrections are made for the diffusional contributions that lead to a finite density of states at $\nu$=0. This provides a rigorous determination of $A$, $S^0$, and other thermodynamic properties from short (20ps) molecular dynamics (MD) trajectories. We used the last 100 ps of the MD trajectories at each temperature. To get a provide statistics we performed our calculations for five separate 20 ps intervals of the MD trajectories.

**Calculation of S1 and S2 splitting.** We computed the position and the splitting between the first (S1) and second (S2) peaks of the structure factor using the atomic coordinates of the water molecules in our MD simulations. We used the LiquidLib program code and formulations for these calculations[7]. We used trajectories from the last 20 ps of 0.5 ns equilibration.

## 2. Primitive Ring Analysis

There have been many advances in improvement and development of methodologies for performing ring analysis to provide important information about the topological networks in materials[8-14]. Ring statistics go beyond the first and second coordination shells to provide details of the network in the intermediate and long range orders in amorphous systems.

There are several ways to define a ring. The first method uses the King criterion[11] which defines a ring based on the shortest path that comes back to the node (i.e. water molecule) through one of its nearest neighbors (Fig. S1). The second method uses a shortest path (SP) criterion[8, 10] where a ring is defined based on the shortest path the connects the two nearest neighbors (Fig. S1).

The maximum number of rings with different sizes ($RDS_{max}$) in the system can be estimated by the King method using

$$RDS_{max}(King) = N(W_n) - 1, \quad (1)$$

or by shortest path (SP) method using

$$RDS_{max}(SP) = \frac{N(W_n)[N(W_n) - 1]}{2}, \quad (2)$$

where $N(W_n)$ is the number of neighbors of molecule $W_n$.

It is also possible to compute the largest size of the ring (RL) based on the above two criteria using

$$RL(King) = 2\ L_{max}, \quad (3)$$

and

$$RL(SP) = 2\ (L_{max} - 1)[N_{max} - 1], \quad (4)$$

where $L_{max}$ is the longest hydrogen bond path that connects two water molecules in the system and $N_{max}$ is the average number of water neighbors for molecules with highest coordination number. We found a value of RL=20 for the system used in this study.

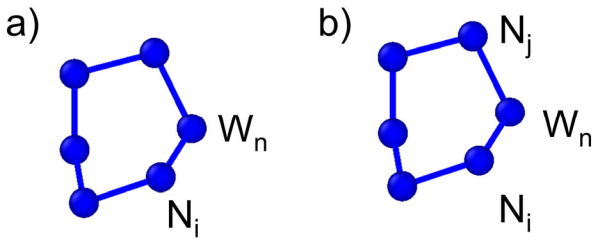


**Fig. S1**. Ring analysis using a) King's and b) shortest path (SP) criteria. In King's criterion a ring is defined based on the shortest path that comes back to the starting node ($W_n$) via the nearest neighbor ($N$). In SP, the ring is defined based on the shortest path between two nearest neighbors ($N_i$ and $N_j$) for $W_n$.

In the present work, we considered only primitive rings to find the correct contribution of water molecules in the 2D network. A ring is called primitive or irreducible if it cannot be reduced into two smaller rings[9, 14]. For example, let's consider the three paths ($I$, $J$, and $K$) provided in Fig. S2. Here, if three path have the same lengths ($L_I$=$L_J$=$L_K$) then the rings $IJ$, $IK$, and $JK$ are all primitive rings. If $L_I$=$L_J$<$L_K$, then there are one smaller ring ($IJ$) and two larger ones ($IK$ and $JK$) but none of them are reducible and therefore the three rings are again primitive. However, if $L_I$<$L_J$=$L_K$ or $L_I$<$L_J$<$L_K$ then the smallest paths is $I$ and the ring $JK$ can be reduced to smaller rings ($IJ$ and $IK$) which means $JK$ is not primitive ring. Further details are provided elsewhere[14].

The neighbors and connectivity tables are computed based on strong hydrogen bond (SHB) analysis using $R_{OO}$<2.93 Å for all molecules of the system. For all ring analyses the periodic boundary condition were considered to account for the images of the molecules. All of the primitive ring analysis were performed using the R.I.N.G.S package[14]. We performed and averaged the ring analysis results over 5 separate intervals (each 20 ps) of the last 100 ps of the MD trajectories at each temperature.

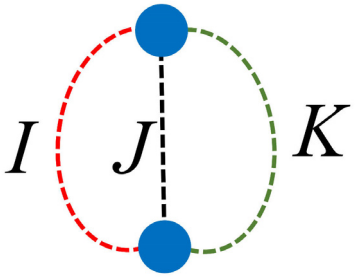


**Fig. S2**. Primitive rings analysis. The rings *IJ*, *IK*, and *JK* are all primitive rings if $L_I=L_J=L_K$ *or* $L_I=L_J<L_K$. If $L_I<L_J=L_K$ or $L_I<L_J<L_K$ then ring *JK* can be decomposed to smaller rings (*IJ* and *IK*) which means *JK* is not primitive.

## 3. Ring Structures of Supercooled Water at Different Temperatures

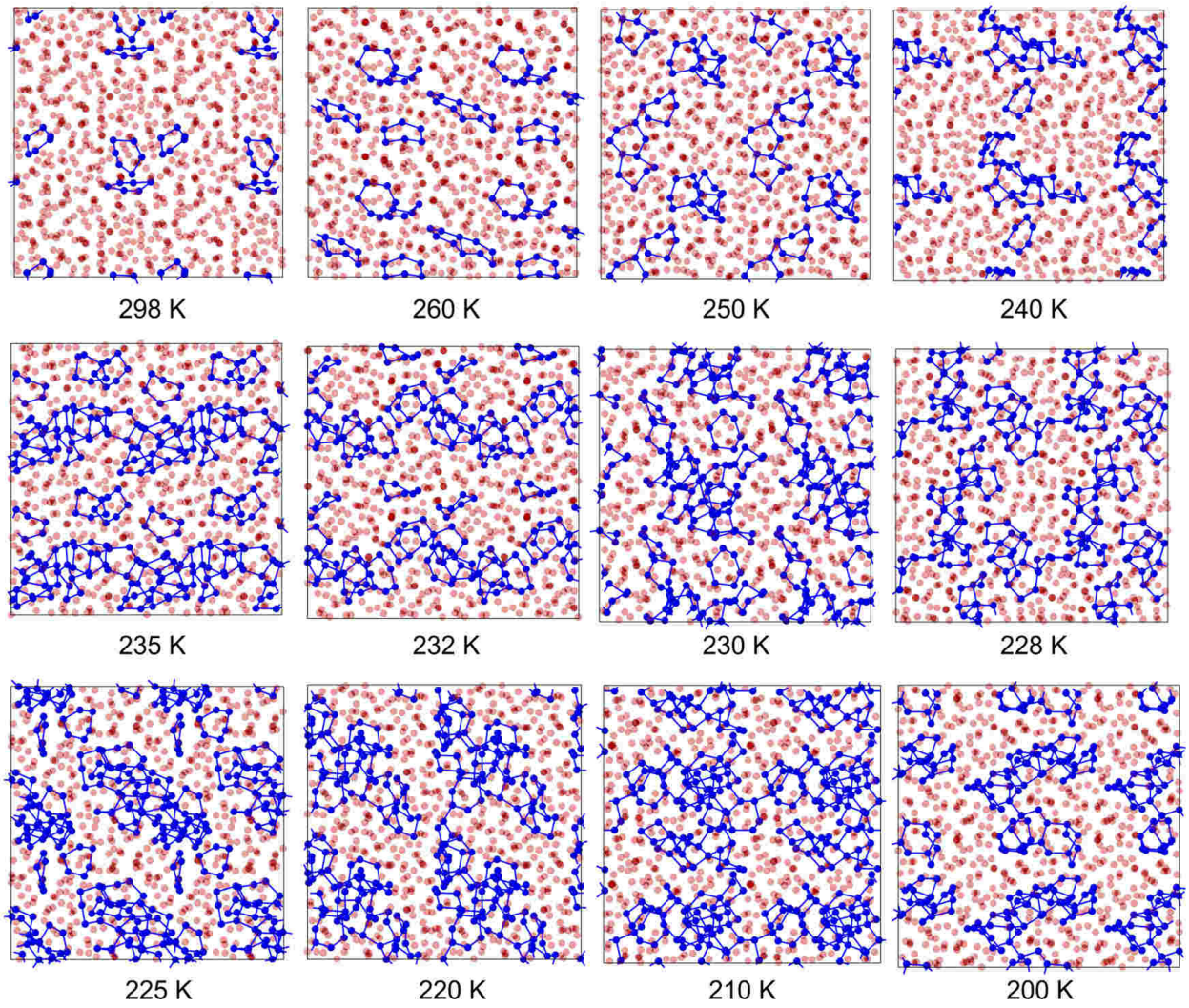


**Fig. S3.** The structure of the 6-membered rings (blue color) in the simulation cells are shown for the temperature range of 298 K to 200 K. Molecules that do not belong to rings are shown with transparent red color. The 6-member rings show clearly the transformation in the structure of supercooled water. The ring formation rate accelerates below 240K leading to a topological transformation to the 2D network by 228 K. The population of molecules in the 2D network is shown better in Fig. S5 which includes the 5, 6, and 7-memembered rings. We selected particular frames that contain the same number of 6-member rings as the average number over the last 20 ps of the trajectory at each temperature. The simulation cells were duplicated along x-, y-, and z-directions to show the connectivity of the bonds and rings to the periodic images.

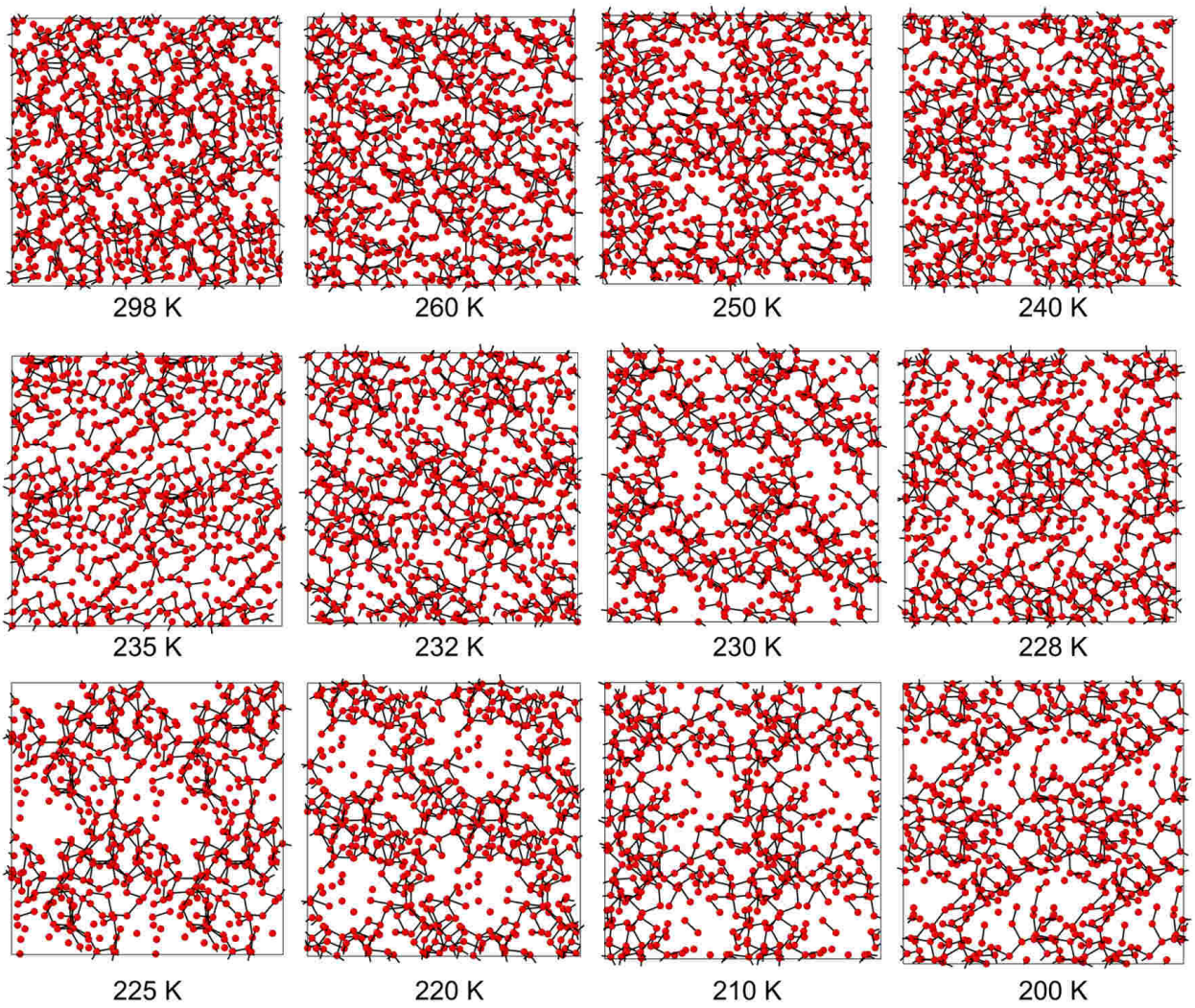


**Fig. S4.** Same as Fig. S3 but now showing only the molecules that do *not* belong to the 6-membered rings. Here, some of the molecules may belong to other ring sizes. The rest of molecules mainly belong to the polymer chains with occasional branch points.

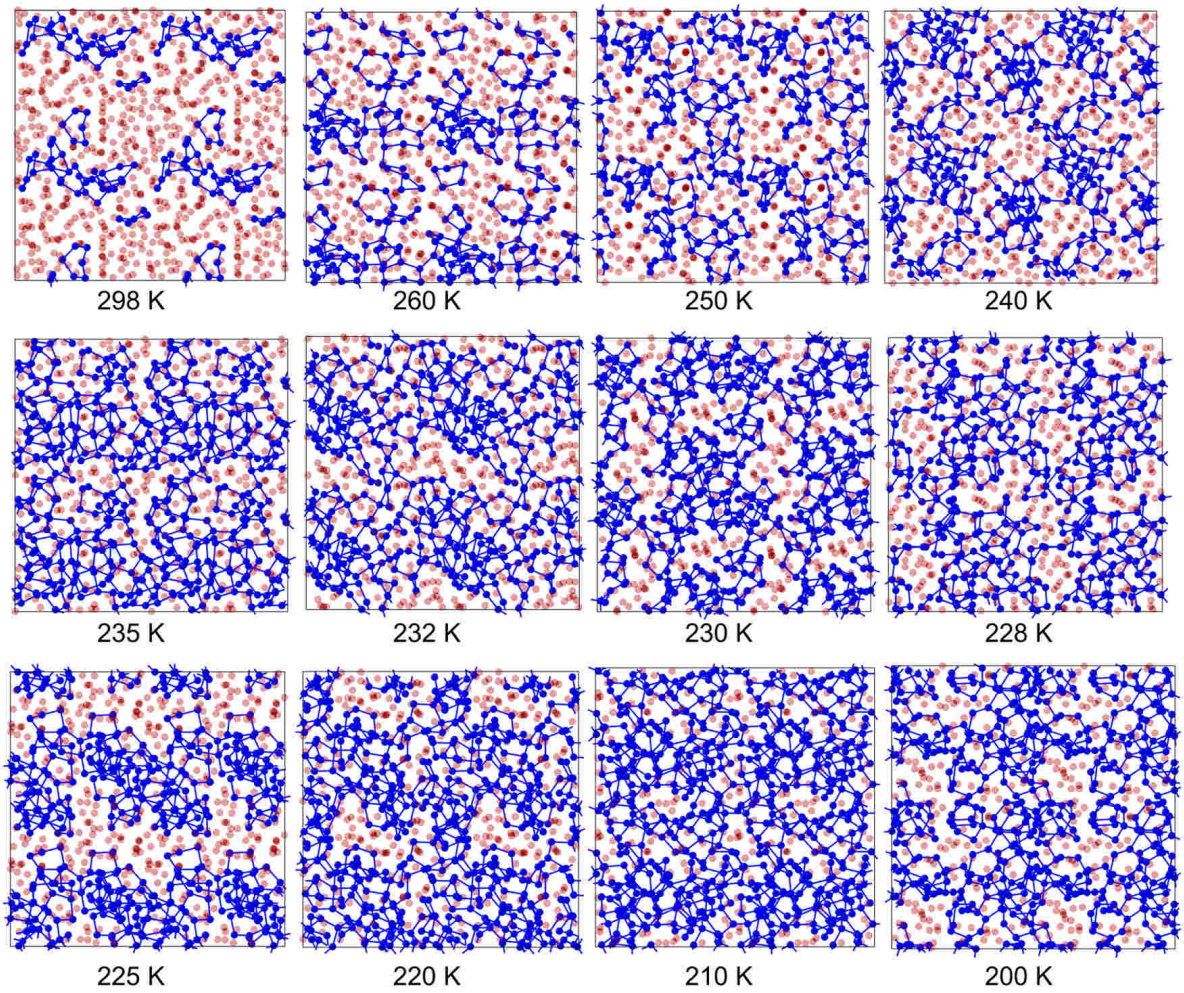


**Fig. S5.** The structure of the 5, 6, and 7-membered rings (blue color) are shown in the simulation cells for the temperature range of 298 K to 200 K. Molecules that do not belong to rings are shown with transparent red color. Few molecules belong to such rings at room temperature (~19%) but as the temperature is decreased the number of molecules in the rings increases to 52% at 230 K and 66% at 220 K (see Table S1 for more details). We selected particular frames that contain the same number of 6-member rings as the average number over the last 20 ps of the trajectory at each temperature. The simulation cells were duplicated along x-, y-, and z-directions to show the connectivity of the bonds and rings to the periodic images.

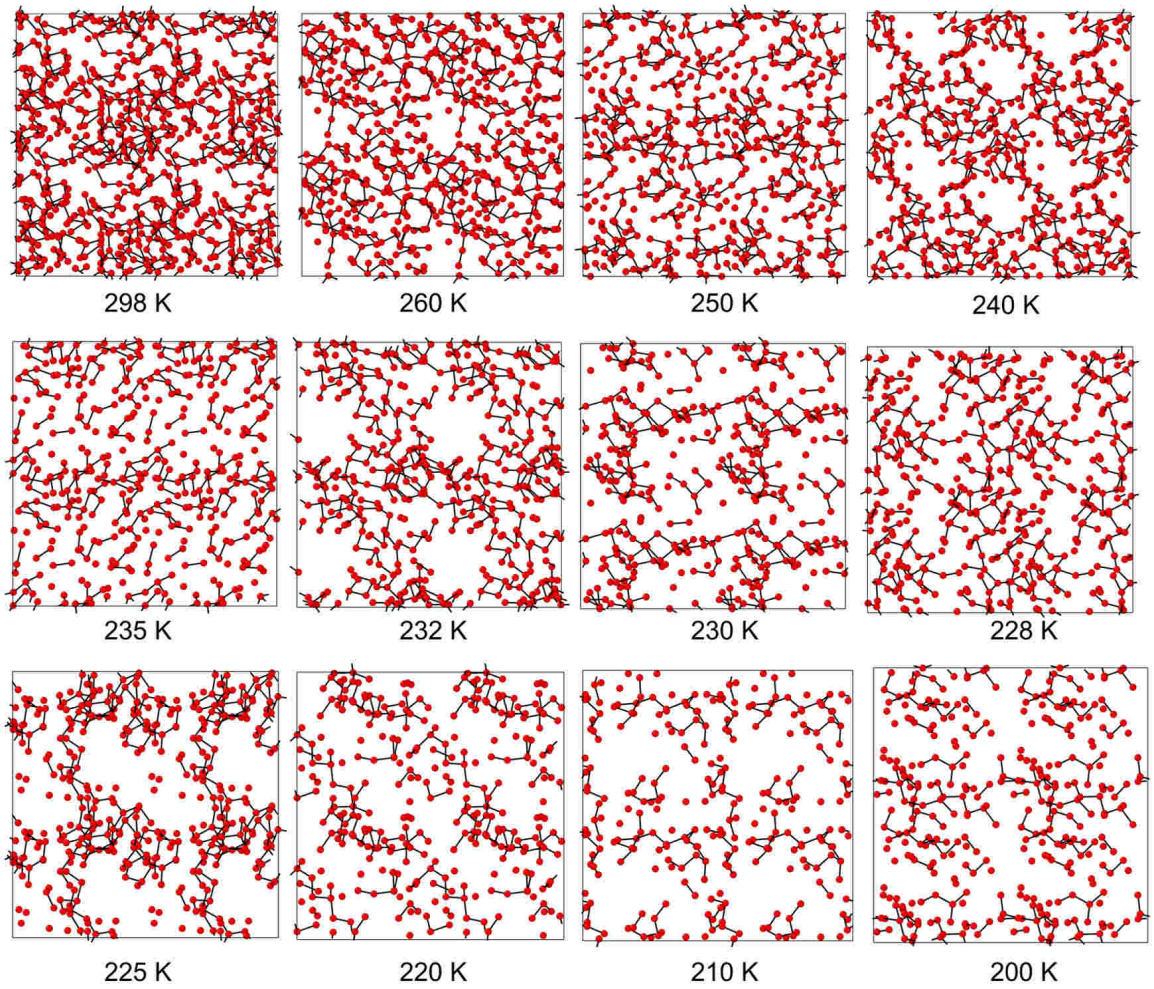


**Fig. S6.** Same as Fig. S5 but showing only the molecules that do not belong to 5, 6, and 7-membered rings. Here, some of the molecules may belong to other ring sizes. As shown, at temperatures below 230 K there are much less number of molecules that are part of 1D polymer chains. These small polymer chains are small fragments with occasional branches.

## 4. Number of Rings of Supercooled Water at Different Temperatures

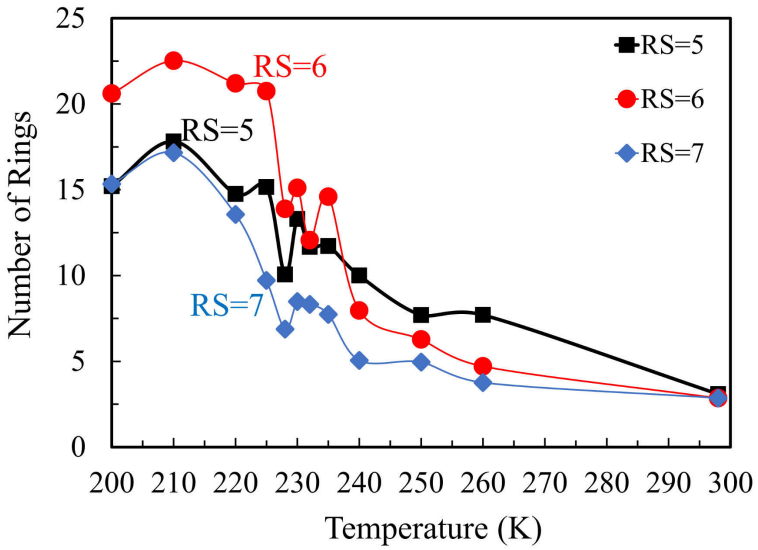


**Fig. S7.** The number of 5-, 6-, and 7-memeberd rings as a function of temperature for supercooled water. For all cases the number of rings increases as the temperature is decreased. But there is a jump in the number of rings in the 228 K to 235 K interval where the topological transformation takes place. Note that there are more 5-membered rings than 6-membered rings for temperatures above ~230 K but below 230 K the 6-membered rings dominate. Below 220 K the number of rings changes little with temperature, showing the relative stability of the 2D network formed.by 220K

## 5. Structural Ordering as a Function of Temperature

We computed the position and the splitting between the first (S1) and second (S2) peaks of the structure factor as the temperature is deceased. We used the trajectories from the last 20 ps (of 0.5 ns equilibration) to compute the structure factor directly from the atomic coordinates of atoms. The computed splitting between S1 and S2 by RexPoN is compared with experimental data of Sellberg *et al*. [15] in Figure 6a of the paper. Since RexPoN provides a good agreement for the splitting (Δq) and position of S1 and S2, it can be used to provide a direct relation between $g_2$ and Δq. In Fig. S8, we plot the $g_2$ values versus Δq to show this trend.

In Figure 6b of the paper, we compare the experimental and computed height of the second peak of $g_{OO}$ ($g_2$) at different temperatures. We interpret the close similarity with the experimental $g_2$ data as an additional validation of the transformation from a 1D polymer into a 2D network at ~230 K (see paper for more discussion). However, the small difference between experiment and RexPoN below 230 K is due to the fact that experiment used TIP4P/2005 water model to create a mapping of the height of $g_2$ versus $\Delta q$ and then used this mapping to estimate the height of $g_2$ from their splitting measurement. Therefore, the experimental $g_2$ values are affected by the inaccuracy of TIP4P/2005 model.

Similar to S1 and S2 curves, Sellberg *et al.*[15] find fluctuations from 232 K to 228 K in $g_2$ curve. Figure 6b of the paper shows similar fluctuations for RexPoN $g_2$ in this region. Fig. S8b suggests that extrapolation of RexPoN $g_2$ value from 200 K to 140 K would meet the experimental $g_2$ for low-density amorphous ice (LDA) from Finney *et al*[16].

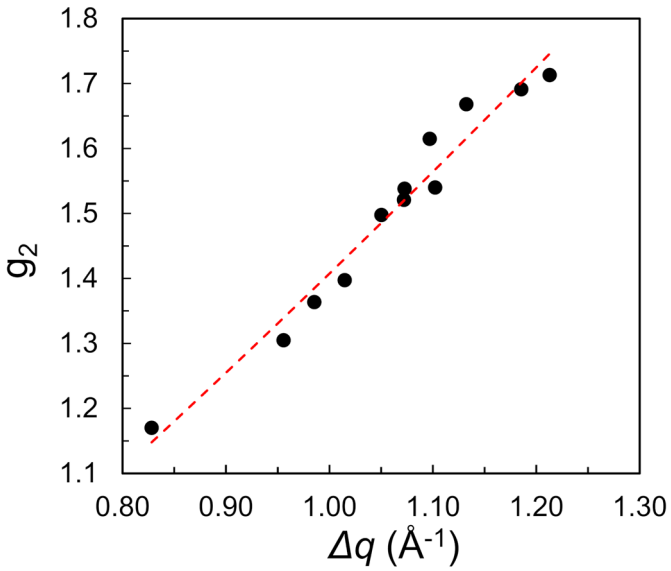


**Fig. S8.** The height of the second peak of oxygen-oxygen radial distribution function ($g_{OO}$) as a function of the splitting (Δq) between S1 and S2 peaks computed by RexPoN. The dotted line is a fit to a second order polynomial to better show the trend of data.

## 6. Structural Analysis of Supercooled Water at 140 K

The point of this paper is to address the anomalous behavior of water at 230 K, so we performed our simulations in the range of 300 to 200 K. However, at low-enough temperatures one might expect that water look like a distorted tetrahedral structure which means a potential 2D to 3D network transition as temperatures is decreased. To check this, we performed RexPoN simulations for the low density amorphous ice (LDA) structure using the experimental temperature of 140 K and density of 0.94 gr/cm$^3$ [17]. Here, we started from the equilibrated structure at 200 K and deformed the cell via constant volume and temperature (*NVT*-MD) simulations to the 0.94 gr/cm$^3$ during 100 ps. Then, we decreased the temperature slowly to 140 K over 1 ns using *NVT*-MD simulations. Finally, we relaxed the structure at 140 K for another 0.5 ns.

We performed the SHB analysis on the last 20 ps trajectories. We added the percent population of each ∑SHB at 140 K to the Fig. 1a of the paper and the results are shown here in Fig. S9. As shown the maximum in ∑SHB changes from ~3.0 at 200 K to ~3.8 at 140 K. This means that the 2D network at 200 K has moved toward a more or less 3D network (perhaps a distorted tetrahedral structure) at 140 K.

However, to confirm these results one would need to run simulations with much larger cells and longer time scales due to much longer relaxation time required for the 2D network.

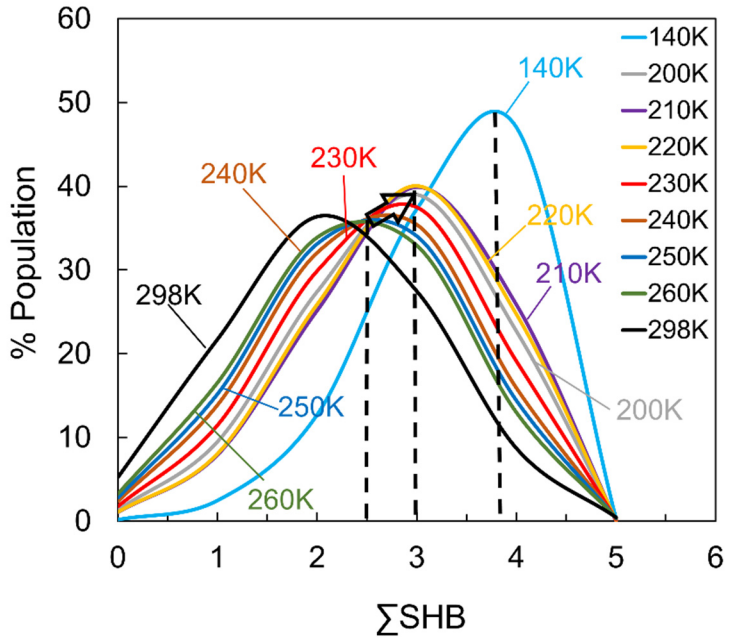


**Fig. S9**. Same as Fig. 1a of the manuscript but added the data for 140 K.

## 7. Diffusivity Calculations for Supercooled Water

Figure 5ab of the paper shows the change of diffusivity versus temperature plotted on both linear and semi-log scales for flexible $D_2O$ molecules. The main message is that the diffusivity is large and increases with temperature above 240K and that it is small with little change with temperature below 220k showing the dramatical effect of the 1D to 2D transformation at ~230K.

Overall, we find good qualitative agreement between the diffusivity change and activation energy as a function of temperature with experiment. We attribute the large fluctuations in the range of 225 K to 235 K as a symptom of 1D to 2D topological transition.

For flexible water simulations, we started from the last frame trajectory of the well equilibrated rigid water system at each temperature and continued the simulations for another 0.5 ns using completely flexible OH bonds and HOH angles. We used heavy water ($D_2O$) to minimize any artifacts in the dynamics due to classical dynamics with hydrogen atoms (and because it is faster since we can use a time step of 1.0 fs). Then, we used 2PT methodology to compute diffusivities.

We find the same qualitative behavior and 1D to 2D topological transition when rigid water molecules are used. However, the rigid water model consistently overestimates the diffusivity (see Fig. S10). The reason is in the rigid water simulations the contribution of OH and HOH vibrations are not included toward the calculation of total diffusivity.

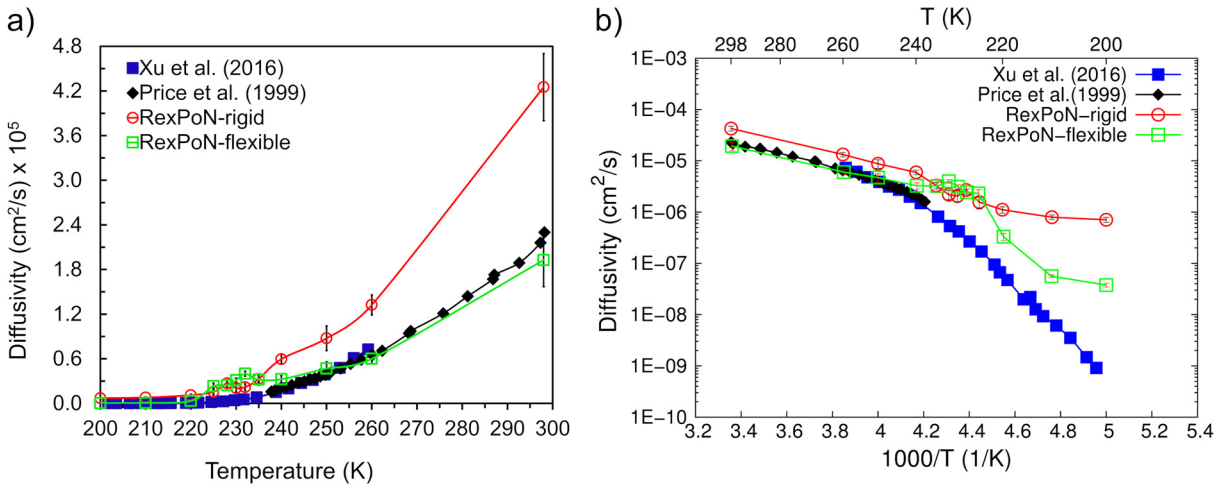


**Fig. S10**. Same as Fig. 5 of the manuscript but the computed diffusivities from rigid RexPoN simulations (red curve) have been added to the plot.

As discussed in the manuscript, we find rapid fluctuations in the structure over the temperature range of 225 to 235 K because different regions are fluctuating between 1D and 2D topologies. This leads to an overestimation of the diffusivity. To get converged diffusivities in this region we probably need a larger unit cell to accommodate all fluctuations within one cell.

To ensure these fluctuations are not due to the use of 2PT methodology, we performed additional MD simulations with RexPoN to compute diffusivities based on mean squared displacements (MSD). We utilized the simulations for the temperature range of 210 to 250 K where fluctuations occur.

For each temperature in this range, we continued the *NVT*-MD simulations for another 1 ns. We computed the diffusivity ($D_S$) from the MSD curve using the three dimensional diffusion equation of Einstein

$$MSD(t) = \lim_{t\to\infty} \langle |r_i(t) - r_i(t_0)| \rangle^2 = 6D_S t \quad (5)$$

where $r_i(t)$ is the position of particle $i$ at time $t$ and $t_0$ is the time origin which can be any time during the simulation. To determine that the simulations were sufficiently long to be Fickian, we show the log MSD versus log time in Fig. S11B. This shows that by about 300 ps all systems have reached the Fickian regime with a slope of 1.0, satisfying $\log(MSD) = \log(t) + \log(6D_{MSD})$. These new $D_S$ from MSD were added to the Figure 5a of the manuscript and the results are shown here in Fig. S12 (RexPoN-MSD).

The computed $D_S$ by MSD follows a similar trend as the diffusivity using 2PT methodology, but with smaller fluctuations in the diffusivities over the temperature range of 225 to 235 K. These results suggest that the fluctuations arise near 1D to 2D transformation. As discussed in the manuscript, we believe that the difference between the magnitudes of computed and measured diffusivity at 220 K and lower is mainly due the nuclear quantum effects (NQE).

We want to emphasize that the empirical models adjusted to reproduce the experimental diffusivity data do not necessarily provide a correct description of the physics of water molecules at the atomistic scale. In addition, nuclear quantum effects (NQE) play an important role on the magnitude of diffusivity at very low temperatures. Therefore, the agreement between the magnitude of the diffusivity of empirical FFs and experiment is only accepted if NQE are included during the dynamics and flexible water models are used.

RexPoN FF was developed based solely on ab-initio data without any bias to reproduce any particular experimental property. This makes RexPoN much more reliable to study the physics and atomistic behavior of water under the conditions that are not accessible to experiment.

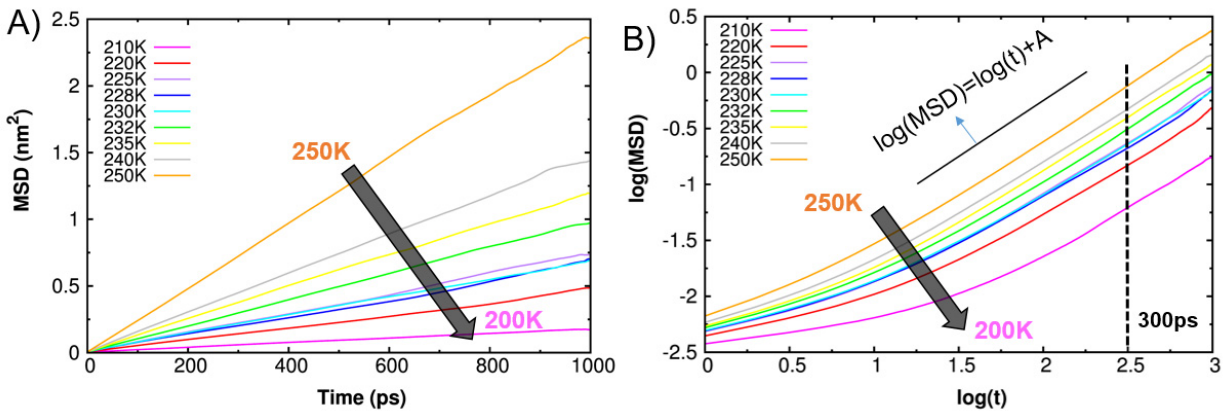


Fig. S11. A) The mean-squared displacement (MSD) with time and B) the logMSD-log time curve with time during 1 ns MD-*NVT* simulations for temperature range of 250 to 200 K. For all temperatures the slope of the log-log curve becomes equal to 1.0 after about 300 ps. The log(MSD)=log(t)+A (black solid line) shows a line with slope 1.0 for reference. Therefore, the slope of the MSD curve after 300 ps is used to determine the self-diffusivity coefficient ($D_s$).

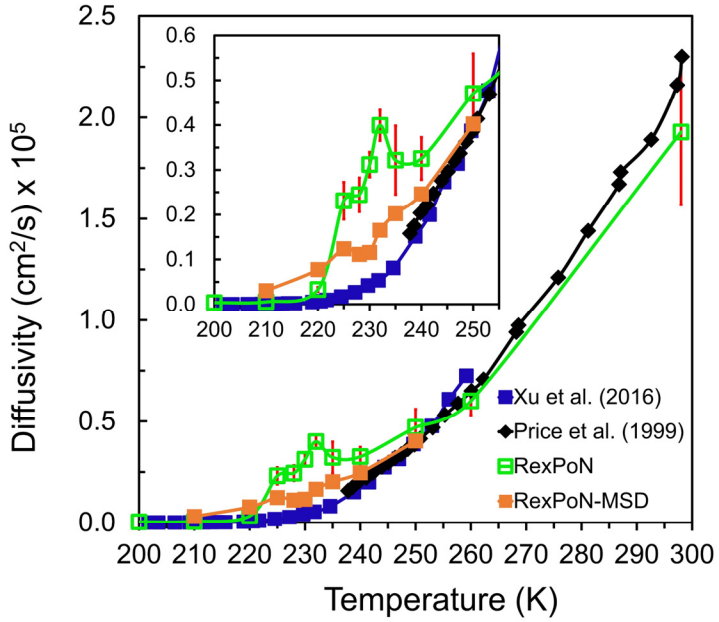


Fig. S12. Same as Figure 5a of the manuscript but the RexPoN diffusivities computed by mean-squared displacement (MSD) method have been added (RexPoN-MSD) for temperature range of 210 to 250 K.

## 8. Hydrogen Bond Lifetime Using Empirical Models

The structure and lifetime of SHB have been the subject of many studies. Regardless of the methodology that is used to describe each of these quantities, the accuracy of the results are directly related to how well the water models are able to describe the first coordination shell of water.

Previously, we compared the oxygen-oxygen radial distribution function ($g_{OO}$) of experiment (Neutron and X-ray), RexPoN, and other water models including the empirical water models of ST2, SPC/E, and TIPnP families[18]. We showed that, other water models leads to a first peak in $g_{OO}$ that differs substantially from the Neutron and X-ray data. Therefore, these models may not provide an accurate description of HB network in water. In fact, the higher first peak by these models result in overestimating the hydrogen bonding due to the larger number of neighbors (the reason that they predict ~4 SHB for water at 298 K).

In our previous work[18], we performed MD simulations of bulk water using SPC/E and TIP4P-2005 water force fields to compute the number of SHB by these models using same Rcut = 2.93 Å criterion that we used for RexPoN. We did this to ensure that the overestimation of SHB by these models is not due to the method that SHBs are computed. Using Rcut = 2.93 Å criterion, we found that all of the water molecules connect to each other through these SHBs to form a distorted tetrahedral structure by these models. Therefore, the overestimation of SHB by these models is indeed due to their inaccuracy to describe the first coordination shell.

This can affect the accuracy of such empirical force fields for predicting other properties of water and ice including the lifetime of HB. For example, in a Nature paper by Matsumoto *et al.* [19] the authors used TIP4P empirical model to study ice nucleation and growth. To do this, they computed the HB lifetime and structure. They found that the lifetime of HB to be 1 ps (1000 fs) at room temperature which is almost 11 times larger than the HB lifetime that RexPoN predicts. This is perhaps due to the extra hydrogen bonds and consequently the tetrahedral structure that TIP4P model predicts for water which results in longer lifetime of HB. This can affect the other computed results from their work.

More of less similar results are found in other studies where empirical models are used to estimate the lifetime of the hydrogen bonds.

In a paper by Prada-Gracia *et al.*[20], the authors reported the HB lifetime of supercooled water at different temperatures. They used different empirical models from SPC and TIPnP families in their simulations. They used similar methodology as we used in this paper and elsewhere[18] to compute the lifetime of HB. They computed the pairwise HB among all water molecules for every frame. For each of the water pairs that formed a bond, the time interval for how long that particular bond survives is called lifetime. They find the HB lifetime of supercooled water to be much larger than RexPoN. At 230 K, they predicted the lifetime to be in the range of 600 fs to 1200 fs much larger than the predicted value of ~125 fs by RexPoN. As mentioned above, we believe that this is because the empirical models overestimate the number of HB in liquid water.

In the study by Stirnemann and Laage[21], the authors used TIP4P-2005 potential to study the non-Arrhenius behavior of water in supercooled region. To do this they combined MD simulation with an analytic extended jump model (EJM) to study the HB dynamics. They defined the jump time as a relaxation time of the HB survival probability. This is the probability that a particular HB has not jumped to a new HB acceptor after a delay time *t*. This HB jump time is essentially different than the HB lifetime that we report by RexPoN or in the above paper by Prada-Gracia *et al.*

Therefore, it is not possible to provide a reasonable comparison between the HB lifetime computed by RexPoN and the above HB jump time. However, the reported jump times for the temperatures in the range of 350 to 235 K are in the range of 13 to 1.5 ps. The authors explain these jump times are much larger than the time required for molecular relaxation (~4 times larger) because the TIP4P-2005 model keeps the water molecules hydrogen-bonded to their 4 closet neighbors (thus they do not experience full relaxation with the first shell). As mentioned above, the extra HB in the TIP4P model probably affect the origin of the non-Arrhenius temperature dependence of liquid waters.

Most important here is the experimental confirmation that used THz pulses on water and examined the echoes[22]. They concluded that the HB lifetimes are 75-90 fs in excellent agreement with our predictions of 90 to 100 fs over the same temperature range.

## 9. Population Analysis of Different Ring Sizes

**Table S1.** The percent population of molecules for different ring sizes (RS) of supercooled water. The population of molecules in the rings increases as the temperature is decreased, which accelerates below 230 K. The number of molecules in RS=5,6,7 reaches to 66.3% at 220 K showing that the majority of the molecules belong to the 2D network for temperatures below the transition temperature (i.e. ~230 K). The molecule is counted only once if it belongs to more than a ring. All values were averaged over 10 ps trajectories with frames at every 1.0 fs.

| T (K) | % (RS=5) | % (RS=6) | % (RS=7) | % (RS=5,6,7) |
|---|---|---|---|---|
| 200 | 28.4 | 39.7 | 33.7 | 64.5 |
| 210 | 31.3 | 42.9 | 36.5 | 69.1 |
| 220 | 30.7 | 39.6 | 31.4 | 66.3 |
| 225 | 24.2 | 32.3 | 22.5 | 54.7 |
| 228 | 19.9 | 27.6 | 18.9 | 49.3 |
| 230 | 25.0 | 26.0 | 20.8 | 51.6 |
| 232 | 26.0 | 34.8 | 27.0 | 59.4 |
| 235 | 24.2 | 23.1 | 17.3 | 47.4 |
| 240 | 17.7 | 20.2 | 15.3 | 41.5 |
| 250 | 18.2 | 20.4 | 14.5 | 41.5 |
| 260 | 15.6 | 11.5 | 10.5 | 31.4 |
| 298 | 6.6 | 7.1 | 7.9 | 18.8 |

## 10. Lifetime of Different Ring Sizes

**Table S2.** The lifetime of different ring sizes ($\tau_{RS}$) for supercooled water. The $\tau_{RS}$ increases slightly as the temperature is decreased but it stays between 20 fs to 40 fs at all temperatures. The average value of $\tau_{RS}$ is 32 fs for RS=5, 27 fs for RS=6, and 22 fs for RS=7. All values were averaged over 10 ps trajectories with frames at every 1.0 fs for each temperature.

| T (K) | $\tau_{RS=5}$ (fs) | $\tau_{RS=6}$ (fs) | $\tau_{RS=7}$ (fs) |
|---|---|---|---|
| 200 | 36.8 | 35.9 | 26.1 |
| 210 | 39.9 | 32.1 | 27.5 |
| 220 | 36.3 | 35.9 | 25.4 |
| 225 | 33.4 | 31.0 | 21.1 |
| 228 | 30.8 | 27.1 | 21.2 |
| 230 | 32.2 | 26.9 | 20.9 |
| 232 | 30.2 | 28.3 | 23.8 |
| 235 | 34.1 | 29.0 | 21.1 |
| 240 | 30.5 | 22.9 | 19.2 |
| 250 | 27.8 | 24.8 | 19.5 |
| 260 | 28.3 | 20.6 | 17.6 |
| 300 | 21.9 | 20.9 | 20.3 |

## 11. References for SI Reference Citations


(1) Naserifar, S.; Goddard III, W. A., The Quantum Mechanics-Based Polarizable Force Field for Water Simulations. *J. Chem. Phys.* **2018**, *149*, 174502.

(2) Plimpton, S., Fast Parallel Algorithms for Short-Range Molecular Dynamics. *J. Comput. Phys.* **1995**, *117*, 1-19.

(3) Kim, K. H.; Späh, A.; Pathak, H.; Perakis, F.; Mariedahl, D.; Amann-Winkel, K.; Sellberg, J. A.; Lee, J. H.; Kim, S.; Park, J., Maxima in the Thermodynamic Response and Correlation Functions of Deeply Supercooled Water. *Science* **2017**, *358*, 1589-1593.

(4) Nosé, S., A Unified Formulation of the Constant Temperature Molecular Dynamics Methods. *J. Chem. Phys.* **1984**, *81*, 511-519.

(5) Lin, S.-T.; Maiti, P. K.; Goddard III, W. A., Two-Phase Thermodynamic Model for Efficient and Accurate Absolute Entropy of Water from Molecular Dynamics Simulations. *J. Phys. Chem. B* **2010**, *114*, 8191-8198.

(6) Pascal, T. A.; Schärf, D.; Jung, Y.; Kühne, T. D., On the Absolute Thermodynamics of Water from Computer Simulations: A Comparison of First-Principles Molecular Dynamics, Reactive and Empirical Force Fields. *J. Chem. Phys.* **2012**, *137*, 244507.

(7) Walter, N. P.; Jaiswal, A.; Cai, Z.; Zhang, Y., Liquidlib: A Comprehensive Toolbox for Analyzing Classical and Ab Initio Molecular Dynamics Simulations of Liquids and Liquid-Like Matter with Applications to Neutron Scattering Experiments. *Comput. Phys. Commun.* **2018**, *228*, 209-218.

(8) Franzblau, D., Computation of Ring Statistics for Network Models of Solids. *Phys. Rev. B* **1991**, *44*, 4925.

(9) Goetzke, K.; Klein, H.-J., Properties and Efficient Algorithmic Determination of Different Classes of Rings in Finite and Infinite Polyhedral Networks. *Journal of non-crystalline solids* **1991**, *127*, 215-220.

(10) Guttman, L., Ring Structure of the Crystalline and Amorphous Forms of Silicon Dioxide. *Journal of non-crystalline solids* **1990**, *116*, 145-147.

(11) King, S. V., Ring Configurations in a Random Network Model of Vitreous Silica. *Nature* **1967**, *213*, 1112.

(12) Wooten, F., Structure, Odd Lines and Topological Entropy of Disorder of Amorphous Silicon. *Acta Crystallogr. Sect. A: Found. Crystallogr.* **2002**, *58*, 346-351.

(13) Yuan, X.; Cormack, A., Efficient Algorithm for Primitive Ring Statistics in Topological Networks. *Computational Materials Science* **2002**, *24*, 343-360.

(14) Le Roux, S.; Jund, P., Ring Statistics Analysis of Topological Networks: New Approach and Application to Amorphous Ges2 and Sio2 Systems. *Computational Materials Science* **2010**, *49*, 70-83.

(15) Sellberg, J. A.; Huang, C.; McQueen, T. A.; Loh, N.; Laksmono, H.; Schlesinger, D.; Sierra, R.; Nordlund, D.; Hampton, C.; Starodub, D., Ultrafast X-Ray Probing of Water Structure Below the Homogeneous Ice Nucleation Temperature. *Nature* **2014**, *510*, 381.

(16) Finney, J.; Hallbrucker, A.; Kohl, I.; Soper, A.; Bowron, D., Structures of High and Low Density Amorphous Ice by Neutron Diffraction. *Phys. Rev. Lett.* **2002**, *88*, 225503.

(17) Jenniskens, P.; Blake, D. F., Structural Transitions in Amorphous Water Ice and Astrophysical Implications. *Science* **1994**, *265*, 753-756.

(18) Naserifar, S.; Goddard, W. A., Liquid Water Is a Dynamic Polydisperse Branched Polymer. *Proc. Natl. Acad. Sci.* **2019**, *116*, 1998-2003.

(19) Matsumoto, M.; Saito, S.; Ohmine, I., Molecular Dynamics Simulation of the Ice Nucleation and Growth Process Leading to Water Freezing. *Nature* **2002**, *416*, 409.
(20) Prada-Gracia, D.; Shevchuk, R.; Rao, F., The Quest for Self-Consistency in Hydrogen Bond Definitions. *J. Chem. Phys.* **2013**, *139*, 084501.
(21) Stirnemann, G.; Laage, D., Communication: On the Origin of the Non-Arrhenius Behavior in Water Reorientation Dynamics. *J. Chem. Phys.* **2012**, *137*, 031101.
(22) Sidler, D.; Meuwly, M.; Hamm, P., An Efficient Water Force Field Calibrated against Intermolecular Thz and Raman Spectra. *J. Chem. Phys.* **2018**, *148*, 244504.